Composition and electronic structure of hidden nanoscale phases and layers of $BaSi_2$ formed in the near-surface of Si

© *B.E. Umirzakov*[1], *M.T. Normuradov*[2], *D.A. Normurodov*[2], *I.R. Bekpulatov*[1]

[1] Tashkent State Technical University,
100095 Tashkent, Uzbekistan
[2] Karshi State University,
180103 Karshi, Uzbekistan

E-mail: be.umirzakov@gmail.com

Received December 29, 2021
Revised January 10, 2022
Accepted January 10, 2022

For the first time, nanoscale phases and layers of $BaSi_2$ were obtained by implantation of Ba^+ ions with an energy of $E_0 = 20-30$ keV in the surface layer of Si(111). In particular, it is shown that at a dose of $D \approx 10^{15}\,cm^{-2}$ nanophases with a band gap $E_g \approx 0.85$ eV are formed, and at $D \approx 10^{17}\,cm^{-2}$ a $BaSi_2$ nanolayer with $E_g = 0.67$ eV. The composition and structure of the barium disilicide nanostructure were investigated by light absorption spectroscopy by Auger electron spectroscopy, and the X-ray surface morphology was studied by scanning electron microscopy. The optimal modes of ion implantation and annealing for obtaining nanoscale phases and layers of $BaSi_2$ in the near-surface region of Si have been established. Using the method of light absorption spectroscopy, the band gap and the degree of coverage of the layer with $BaSi_2$ nanophases were estimated. It has been shown that at a dose of $D \geq 6 \cdot 10^{16}\,cm^{-2}$ the nanolayer of $BaSi_2$.

Keywords: ion implantation, nanostructure, nanophase, annealing, barium disilicide, Auger electrons, degree of coverage.

DOI: 10.21883/SC.2022.05.54732.9795

1. Introduction

Multilayer thin-film nanostructures containing layers of $NiSi_2$, $CoSi_2$ and other metal silicides are promising in the creation of MIS (metal-insulator–semiconductor), SIS (semiconductor-insulator–semiconductor) structures, ohmic contacts and barrier layers at the phase boundary between these structures, electronic and magnetic storage devices. Therefore, in recent years there has been the sharp increase in interest in obtaining and studying the properties of nanoscale semiconductor superlattices based on Si [1–9]. Such structures are usually created by the method of molecular beam epitaxy (MBE). Moreover, as the results of the study by Auger electron spectroscopy (AES) and low-energy electron diffraction (LEED) showed, the formation of chemical compounds begins with doses exceeding the critical dose of Si surface amorphization for this type of ions. In particular, the authors of the works [10–12] showed that barium disilicide on silicon, due to its optical properties, photovoltaic characteristics and resistance to atmospheric air, is a promising material for photoelectronic converters in the solar energy range.

One of the promising methods for creating nanoscale structures on the surface and in the near-surface region of semiconductor and dielectric films is the method of ion implantation [13,14]. In particular, in the work [14], the composition, structure and E_g of nanophase and nanolayers of $CoSi_2$ formed in the near-surface Si layer at the depth of $15-30$ nm were obtained and studied. Ion implantation allows not only to introduce impurities to the required depths in the required amount, but also leads to the spraying of foreign impurities (oxygen, carbon, etc.) from the surface area of the substrate [15–20].

In this work, we first tried to obtain nanoscale phases of the $BaSi_2$ at various depths of Si and create nanoscale heterosystems of the $Si/BaSi_2/Si$ type.

2. Procedure

Implantation of Ba^+ ions, heating of samples, investigation of their composition and parameters of energy bands using AES methods and measurement of the intensity of light passing through the sample were carried out in the same device under ultrahigh vacuum conditions ($P = 10^{-7}$ Pa). The surface morphology was studied by scanning electron microscopy SEM (*Jeol*).

Nanoscale phases and layers of $BaSi_2$ in various depths of the near-surface layer of Si were obtained by implantation of Ba^+ ions with energy variation E_0 within limits of $20-40$ keV and dose $D = 10^{14}-10^{17}\,cm^{-2}$, at vacuum no worse 10^{-7} Pa.

3. Results and discussion

Figure 1 shows the concentration profiles of the distribution of Ba in depth h for Si(111) implanted with Ba^+ ions with $E_0 = 20$ keV at the saturation dose of $D \approx 10^{17}\,cm^{-2}$ before and after warming up at $T = 950$ K within the period of 40 min.

Optimal modes of ion implantation and annealing for obtaining nanocrystals (NC) BaSi$_2$ at various depths of Si (111)

Subject of study	$E_0 = 20\,\text{keV}$				$E_0 = 30\,\text{keV}$			
	D, cm^{-2}	T, K	d, nm	h, nm	D, cm^{-2}	T, K	d, nm	h', nm
$Ba^+ \rightarrow Si(111)$	$5 \cdot 10^{14}$	950	6–8	16–18	$5 \cdot 10^{14}$	950	6–8	25–30
	10^{15}	950	8–10		10^{15}	1000	8–10	
	$5 \cdot 10^{15}$	1100	10–12		$5 \cdot 10^{15}$	1100	10–12	

The analysis of Auger spectra showed that the curves pass through the maximum at a depth of $h = 16-18$ nm. The dependence $C_{\text{Ba}}(h)$, measured before warming up, exhibits the broad maximum with concentration of ~ 20 at%. After warming up, there are the concentration of atoms in the maximum region increases to $30-35$ at% and the significant decrease in the half-width of the distribution curve $C_{\text{Va}}(h)$. In this case, the position of the Auger peak of silicon $L_{2,3}VV$ ($E = 92$ eV) is shifted to the energy ~ 96 eV, which is typical for BaSi$_2$. It can be seen from the curve *2* that the width of the layer BaSi$_2$ is $\sim 10-12$ nm. At the boundaries of Si/BaSi$_2$/Si, transition layer with a thickness of $\sim 6-8$ nm is formed, which is significantly larger than in the case of CoSi$_2$/Si/CoSi$_2$ [14].

For this system, Fig. 2 shows the dependence of $I_{\text{BaSi}_2}/I_{\text{Si}}$ on the photon energy $h\nu$, where I_{Si} and I_{BaSi_2} are the intensity of the transmitted light through pure Si(111) and through Si(111) with hidden nanolayer BaSi$_2$, respectively. It can be seen from Fig. 2 that the light intensity of the studied samples up to certain value of $h\nu$ practically does not change. In the case of pure Si, the sharp decrease of I begins with $h\nu \approx 1$ eV, and in the case of Si with the BaSi$_2$ nanolayer — with $h\nu \approx 0.55$ eV. Extrapolation of this part of the curves to the $h\nu$ axis gives the approximate value of the band gap. It can be seen that E_g for pure Si is ~ 1.1 eV, and for BaSi$_2$ — ~ 0.67 eV. After warming up of Si implanted with Ba$^+$ ions with the low dose ($D \leq 5 \cdot 10^{15}\,\text{cm}^{-2}$), regularly arranged nanocrystalline phases BaSi$_2$ are formed in the near-surface layer.

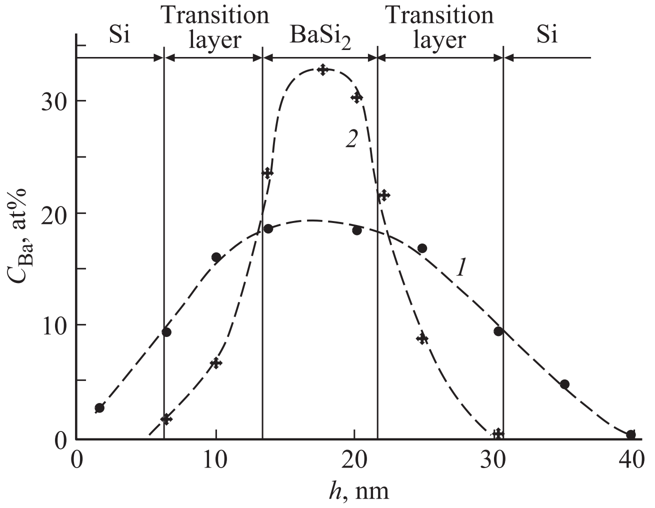

Figure 1. Profiles of the distribution of Ba atoms in depth h for Si implanted with Ba$^+$ ions with energy $E_0 = 15$ keV at $D \simeq 10^{17}\,\text{cm}^{-2}$: *1* — before warming up, *2* — after warming up at $T = 900$ K $I_{\text{BaSi}_2}/I_{\text{Si}}$.

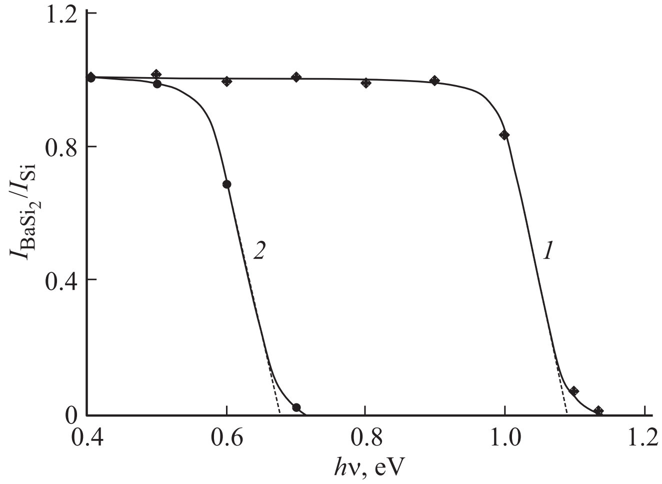

Figure 2. The dependence of the intensity of the transmitting light on the photon energy for pure Si (curve *1*), and Si with the nanolayer BaSi$_2$ (curve *2*).

The table shows the optimal modes of ion implantation and annealing for obtaining of NC BaSi$_2$ in two different depths of the Si(111) single crystal. After each ion implantation cycle, the sample was warmed up at the appropriate temperature within the period of 30 min.

It can be seen from the table that after warming up of Si implanted with Ba$^+$ ions with $E_0 = 30$ keV, nanocrystalline phases in the form of spheres were formed at a depth of 25–30 nm. In both cases up to $D \approx 10^{15}\,\text{cm}^{-2}$ these phases have the shape close to spherical. With further growth D, the boundaries of neighboring phases overlap each other and layers of BaSi$_2$ begin to form. However, the uniform thickness layer of BaSi$_2$ is formed at $D \approx 10^{17}\,\text{cm}^{-2}$.

Figure 3 shows the dependence of $I_{\text{BaSi}_2}/I_{\text{Si}}$ on $h\nu$ for Si with hidden nanophases BaSi$_2$ obtained by implantation of Ba$^+$ ions with $E_0 = 20$ keV at $D = 10^{15}\,\text{cm}^{-2}$. Averaged values of the distance between phases, which

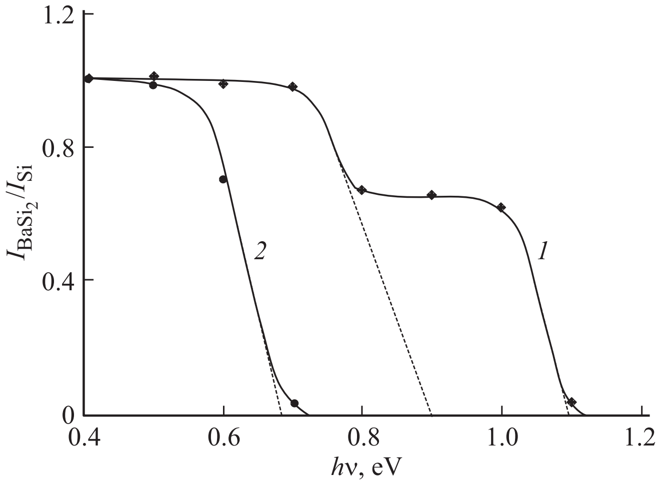

Figure 3. The dependence of the intensity of the transmitting light on the photon energy for Si with the nanophases $BaSi_2$ (curve *1*), and the nanolayer $BaSi_2$ (curve *2*).

were estimated by scanning electron microscopy (SEM) by the means of the image, were $\sim 45-50$ nm. It can be seen that the dependence has the stepwise character and the average value of E_g for $BaSi_2$ nanocrystals is 0.8–0.85 eV, and the relative area of the NC $BaSi_2$ in these layers of Si is $\sim 0.25-0.3$. Thus, varying the ion dose in the range of $\sim 5 \cdot 10^{14}-5 \cdot 10^{15}\,\mathrm{cm}^{-2}$, it is possible to change the volumes of nanocrystalline phases within limits from $\sim 10^{-19}$ up to $10^{-18}\,\mathrm{cm}^3$. In this case, the band gap decreases monotonically from ~ 1 to ~ 0.67 eV. At $D \leq 10^{14}\,\mathrm{cm}^{-2}$, we did not detect the formation of nanocrystalline phases of $BaSi_2$ with good stoichiometry. In addition, due to the low concentration of Ba atoms, the dependence $I(h\nu)$ does not show a noticeable decrease in the intensity of the transmitting light up to the values $h\nu \sim 1$ eV. At $D > 5 \cdot 10^{15}\,\mathrm{cm}^{-2}$, the overlapping of the boundaries of individual cluster phases is observed.

4. Conclusion

The optimal modes of ion implantation and annealing are determined for obtaining hidden nanoscale phases and layers of $BaSi_2$ in the near-surface region of Si. Using the method of light absorption spectroscopy, the band gap and the degree of coverage of the layer with $BaSi_2$ nanophases are estimated. It is shown that at a dose of $D \leq 5 \cdot 10^{15}\,\mathrm{cm}^{-2}$ nanoscale $BaSi_2$ phases are formed, and quantum-size effects are manifested in them. At high doses $D = D_n = 10^{17}\,\mathrm{cm}^{-2}$ the nanolayer of $BaSi_2$ $\sim 10-12$ nm thick is formed.

Conflict of interest

The authors declare that they have no conflict of interest.

References

[1] B. Li, J. Liu. J. Appl. Phys., **105**, 084905 (2009). Doi: 10.1063/1.3110183

[2] V.I. Rudakov, Yu.I. Denisenko, V.V. Naumov, S.G. Simakin. Pis'ma ZhTF, **37** (3), 36 (2011) (in Russian).

[3] V.L. Dubov, D.V. Fomin. Uspekhi prikladnoi fiziki, **4** (6), 599 (2016) (in Russian).

[4] J.Sh. Chai, X.X. Zhu, J.T. Wang. J. Mater. Sci., **55**, 9483 (2020). Doi: org/10.1007/s10853-020-04685-5

[5] D. Tsukahara, S. Yachi, H. Takeuchi, R. Takabe, W. Du, M. Baba, Y. Li, K. Toko, N. Usami, T. Suemasu. Appl. Phys. Lett., **108**, 152101 (2016).

[6] N.G. Galkin, D.L. Goroshko, V.L. Dubov, D.V. Fomin, K.N. Galkin, E.A. Chusovitin, S.V. Chusovitina. Jpn. J. Appl. Phys., **59**, SFFA11 (2020).
Doi: org/10.35848/1347-4065/ab6b76

[7] K.O. Hara, Y. Hoshi, N. Usami, Y. Shiraki, K. Nakamura, K. Toko, T. Suemasu. Thin Sol. Films, **557**, 90 (2014).

[8] Z.Z. Cheng, Z. Cheng, B. Xu. Chin. Phys. Lett., **24** (9), 2649 (2007).

[9] Sh. Kishino, T. Imai, T. Iida, Y. Nakaishi, M. Shinada, Y. Takanashi, N. Hamada. J. Alloys Compd., **428**, 22 (2007).

[10] Kh.Kh. Boltaev, D.A. Tashmukhamedova, B.E. Umirzakov. Poverkhnost. Rentgenovskie, sinkhrotronnye i nejtronnye issledovaniya, **4**, 24 (2014) (in Russian).
Doi: 10.7868/S0207352814010107

[11] B.E. Umirzakov, D.A. Tashmukhamedova, Kh.Kh. Kurbanov. Poverkhnost. Rentgenovskie, sinkhrotronnye i nejtronnye issledovaniya, **7**, 91 (2011) (in Russian).

[12] D.M. Murodkobilov, D.A. Tashmukhamedova, B.E. Umirzakov. Poverkhnost. Rentgenovskie, sinkhrotronnye i nejtronnye issledovaniya, **10**, 58 (2013) (in Russian).

[13] N.V. Alov. Meth. Phys. Res. B, **256** (1), 337 (2007).

[14] Y.S. Ergashov, B.E. Umirzakov. Techn. Phys., **63** (12), 1820 (2018). Doi: 10.1134/S1063784218120058

[15] K. Ivna, J. Piltaverlavana, R. Badovanic. Appl. Surf. Sci., **425**, 416 (2017).

[16] A.S. Risbaev, J.B. Khujaniyazov, I.R. Bekpulatov, A.M. Rakhimov. J. Surf. Investigation: X-ray, Synchrotron and Neutron Techniques, **11** (5), 994 (2017).
Doi: 10.1134/S1027451017050135

[17] I.G. Donskoy. Energy Systems Res., **2** (3), 55(2019).

[18] K. Oura, G.V. Lifshitz, A.A. Saranin, A.V. Zotov, M. Katayama. *Vvedenie v fiziku poverkhnosti* (M., Nauka, 2006), p. 52 (in Russian).

[19] F. Liao, S.L. Girshick, W.M. Mook, W.W. Gerberich, M.R. Zachariah. Appl. Phys. Lett., **86**, 171913 (2005).

[20] J.A. Borders, S.T. Picraux, W. Beezhold. Appl. Phys. Lett., **18** (11), 509 (1971).